Hydrogeophysics contribution to the development of hydrogeological conceptual model of coastal aquifers – Albufeira-Ribeira de Quarteira aquifer case study

Métodos hidrogeofísicos aplicados ao desenvolvimento do modelo hidrogeológico conceptual de aquíferos costeiros – caso de estudo do aquífero de Albufeira-Ribeira de Quarteira

Alain P. Francés[(1)], Elsa C. Ramalho[(1)], Judite Fernandes[(1)], Michel Groen[(2)], Joel de Plaen[(2)], Rui Hugman[(3)], Mohamed A. Khalil[(4)], Fernando A. Monteiro Santos[(4)]

[(1)] LNEG - National Laboratory of Energy and Geology, Apartado 7586 – Alfragide, 2610-999 Amadora, frances.alain@lneg.pt, elsa.ramalho@lneg.pt, judite.fernandes@lneg.pt

[(2)] VU University Amsterdam, Faculty of Earth and Life Sciences, De Boelelaan 1085, 1081 HV Amsterdam, The Netherlands, m.m.a.groen@vu.nl, joel.deplaen@gmail.com

[(3)] UALG - Geo-Systems Centre/CVRM, Universidade do Algarve, 8005-139 Faro, Portugal, rui.hugman@ist.utl.pt

[(4)] IDL - Centro de Geofísica da Universidade de Lisboa, Campo Grande, Ed. C8, 1749-016 Lisboa, Portugal, khalil250@hotmail.com, fasantos@fc.ul.pt

SUMMARY

We applied geoelectrical and electromagnetic (time and frequency domains) hydrogeophysic methods to retrieve the structure of the Albufeira-Ribeira de Quarteira coastal aquifer (Algarve, Portugal) and to update the current hydrogeological conceptual model (HCM). The results allowed detecting the freshwater–saltwater interface along the coast line, identifying the water-bearing layers and aquitards and their hydraulic relationships, as well as explaining the location of the inter- and subtidal freshgroundwater discharge. These results will be integrated further works in a hydrogeophysics-based HCM that will support the setup of variable-density groundwater flow numerical model.

1 INTRODUCTION

Coastal areas concentrate economic activities related to harbors and maritime transport, being also propitious to the development of beach tourism due to a pleasant climate and quality of life. These characteristics explain that they aggregate ~50 % of the world's population and ~75 % in Portugal (Creel, 2003; Presidência do Conselho de Ministros, 2009). Coastal aquifers (CA) generally ensure part or totality of water supply to domestic, agricultural, industrial and tourism sectors. The increase of the permanent population and tourists during the dry season constitute a tremendous pressure on the CA groundwater resources. Besides threats common to any aquifer, such as overexploitation, pollution by waste water or leaching of contaminates, decrease of groundwater recharge due to climate change and soil impermeabilization in urban areas, CA are also vulnerable to seawater intrusion and upconing that provoke fresh water salinization (Dörfliger, 2013; Post, 2005). The protection of the groundwater resource in coastal areas and its sustainable management, in conjunctive use with other water resources (e.g. surface water, desalinized seawater), require the understanding of the CA hydrogeology. Since the late XIX century, hydrogeologists developed tools to study CA, such as analytical models (Dingman, 2002; Fetter, 2001; Oude Essink, 2001), numerical models of variable-density flow and solute transport (Bakker and Schaars, 2005; Langevin et al., 2007), field data acquisition methods including airborne and ground-based geophysics (Auken et al., 2010; Henderson et al., 2010; Kok et al., 2010) and automatic data acquisition systems that allow high-resolution monitoring of groundwater level, temperature and salinity (Dörfliger, 2013; Poulsen et al., 2010). These tools allowed to identify and map CA occurrences (Custodio, 2010 and other papers of the "Saltwater and freshwater interactions in coastal aquifers" issue of Hydrogeology Journal; Fleury et al., 2007), as well as to better understand their dynamic (Aunay et al., 2007; de Montety et al., 2008; Dörfliger, 2013; Post and Abarca, 2010; Werner et al., 2013) and to improve their management (Aunay et al.; Barazzuoli et al., 2008). However, there are still scientific challenges to be solved in order to support the resolution of real world problems. Following Post (2005), these challenges are grouped in: (i) conceptual issues; (ii) mathematical models; and (iii) subsurface characterization. Indeed, the theoretical conceptual model of the steady-state freshwater–saltwater interface (FSWI) is more an exception than a rule. The position of the FSWI is ruled by highly dynamic processes and varies spatio-temporally. This results in some cases in deep submarine groundwater discharge (SGD) and in other cases in continental brackish springs above seawater level. It was showed that the position of the interface and the distribution of fresh and saline groundwater is also a result of sea transgression and regression at long time scale, i.e. hundreds of thousands of years (Fleury et al., 2007; Post, 2005; Post et al., 2013). Multilayer aquifers separated by aquitard and aquiclude, as well as geological settings such as karstification, complicate the theoretical framework. Mathematical models of variable-density groundwater flow may help in understanding the aquifer dynamic and support management decision. Such models require parametric and geometry knowledge of the aquifer obtained by subsurface characterization methods. Subsurface data are generally scarce because invasive methods such as borehole drilling and associated aquifer tests are expensive and time-consuming. Hydrogeophysics provides non-invasive methods of subsurface data acquisition that efficiently complement direct observations. As each method has its own characteristics and capability, their complementary use allows covering a wide range of hydrogeological problems, including the CA specificities.

In this study, we present a hydrogeophysics-based methodology to contribute to the development of CA hydrogeological conceptual model (HCM). Hydrogeophysics methods were applied to: (i) detect the FSWI along the coast line; (ii) identify the water-bearing layers and aquitards and relate them with the geological formations and SGD localization. The hydrogeophysics results were interpreted using complementary information such as boreholes logs, regional static piezometric map and analytical models of the FSWI. We applied this methodology to the Albufeira-Ribeira de Quarteira (ARQ) CA (Algarve, south of Portugal) in the framework of the FREEZE project (PTDC/MAR/102030/2008, FCT founding), which main objectives were to detect and characterize SGD and their impact on submarine ecosystems (Carrara, 2012; Encarnação et al., 2013).

2 METHODOLOGY

The general methodology was composed by two main steps: (i) review of geological and hydrogeological information (maps, reports, thesis and articles) to identify uncertainties related with 3D aquifer structure, hydraulic relationships between geological formations and position of the FSWI; (ii) selection of key-sites where hydrogeophysics methods were carried out to clarify the identified problems. These analyses were complemented with the following auxiliary data: (i) boreholes logs; (ii) hydraulic heads records; (iii) analytical models of the FSWI.

2.1 Study area

The study area is located in the Algarve region, the southernmost province of Portugal, characterized by a warm Mediterranean, semi-arid climate. The Algarve mean annual temperature and precipitation are around 17º C and 600 mm, respectively. The precipitation regime is irregular, having intermittent periods with heavy rains in the winter and a long dry period in the summer.

The southern coast of Portugal is characterized by an important development of the tourism sector, particularly demanding in water supply directly but also indirectly for the irrigation of the numerous hotels, resorts and golf courses flanking the coast of the area. Furthermore the water abstraction for agricultural purpose, such as the irrigated market gardening, represents a significant need of water. The vegetation is mainly composed by citrus tree used for cultivation and other commercially attractive trees such as olive, almond and cork oak trees.

The geomorphology of the Algarve littoral is characterized on the East by a shore line of sandy deposit and the West by a platform forming a cliff well observed between Albufeira and Olhos de Água. Inland, the area can be described as coastal plain with low relief, bordered on the north by jurassic limestone with a more pronounced relief. Several characteristic karstic features can also be observed such as doline and dry valleys.

2.1.1 Geology

The onshore Meso-Cenozoic Algarve basin is an E-W trending sedimentary basin filled by more than 4000 m of sediment lying on Carboniferous schists and greywackes. Discordantly on the paleozoic substratum, sandstones and conglomerates of the "Arenitos de Silves" deposited during the middle to upper Triassic, followed by the "Complexo Pelítico Carbonatado-Evaporítico". This sedimentary cycle ends with a volcanic-sedimentary complex related to the first rifting phase (Manuppella, 1992). These formations with the carboniferous formation constitute an impermeable substratum.

During the Lias, limestones and dolomites (600 m thick) deposited in central Algarve, extending from Lagoa to Tavira. The transition to the Dogger is marked by an erosional phase followed by deposition of oolitic limestones and marls (350 to 500 m of thickness). Lias and dogger formations constitute the most important aquifers of the region since they present good hydraulic properties, large thickness and outcrop extensively (e.g. M5 aquifer in Figure 1). Moreover, these formations have been affected by an intense secondary dolomitization process that produced their high porosity and permeability.

During the Malm, mainly in the upper Oxfordian-lower and middle Kimmeridgian, the variation between sedimentary environments increases due to a second phase of rifting. From the upper Kimmeridgian on, an inner platform environment develops, promoting thick regressive carbonate sequences with maximum expression in the Tithonian-Cretaceous. These formations have good hydrogeological properties and support important aquifers systems, namely ARQ.

The transition to the Cretaceous is marked by a marine and fluvial sedimentation, while in the lower Aptian the subsidence increases and begins a transgressive episode due to the North Atlantic expansion. The lower Cretaceous sediments are composed by marls, limestones, dolostones and a few sandy and conglomeratic levels. Hydrogeologically, they are less favorable than the jurassic formations even if they can support aquifers when sufficiently thick and extended.

The Lagos-Portimão Formation corresponds to deposits of carbonate platform, developed during a long time span (lower Burdigalian to upper Serravallian). Strongly affected by karstification, this formation overlies the carboniferous, jurassic, cretaceous and possible paleogene units with angular unconformity, stratigraphical hiatuses or paraconformaties (Pais et al., 2000). From hydrogeological point of view, this formation is very productive and constitutes an important source for fresh water supply and irrigation. Next, the sedimentation conditions passed from carbonate to siliciclastic environments during the lower Tortonian with the deposition of the Olhos de Água Sands (Pais et al., 2000).

The Faro-Quarteira Sands corresponds to quaternary continental sedimentation of siliciclastic deposits with reddish colors (50 m maximum thickness). This formation covers most of the Algarve region, being largely exploited for irrigation purposes trough traditionally large wells called "noras".

2.1.2 Hydrogeology

The ARQ aquifer system (M6 in Figure 1) was characterized by Almeida and Lourenço da Silva (1990) and Almeida et al. (2000). These last authors defined the limit of the ARQ, as shown in Figure 1, with the aim to define inventory and management units.

The water-bearing formations are composed by detritic-carbonate rocks dating from Miocene and upper Jurassic (Table 1 and Figure 1). The two formations, called from here jurassic and miocenic aquifer respectively, are supposedly separated by the cretaceous aquitard, identified in Figure 2 (right). Structural conditions allow, in some sectors, the contact between the two water-bearing formations, making possible hydraulic connection. Between Albufeira and the Quarteira river, the subtabular Miocene is tilting slightly towards S-SE (Figure 2 right). Miocenic formations sedimented with strong angular unconformity over the cretaceous and jurassic formations (Figure 2 right). They are partly recovered by the plio-quaternary formations that act as an aquitard, confining unit.

The diapir west of Albufeira (Figure 1 and Figure 2 left) was responsible for the strong angular unconformity (near 90°) between the Miocene and Cretaceous. Another not outcropping diapir, but whose presence is denounced by hydrochemical characteristics of the groundwater, is located E of Escarpão, extending southwards to the vicinity of Patã de Baixo, i.e. on the west border of the ARQ, along the Quarteira river.

The aquifer system boundaries are defined by three tectonic major accidents (Figure 1):

- East: the NW-SE Quarteira fault, which conditioned the Miocenic sedimentation since the eastern compartment (M7 aquifer) is thicker (180 m) than the western compartment (80 m, ARQ-M6 aquifer);
- North: W-E Sagres-Algoz-Vila Real de Santo António fault zone (see also Figure 2 left);
- West: N-S Albufeira fault and Albufeira diapir (see also Figure 2 left).

The south boundary is formed by the seacoast. Inter and subtidal springs of fresh to brackish water along the coast line, in particular at Olhos de Água (Figure 1), indicate that ARQ discharges into the sea. Another discharge area is the Quarteira river (Almeida et al. 2000; Reis 2007), although this stream may also be influent.

Transmissivity was estimated in 30 boreholes exploiting the Miocenic formation. It ranges between 84 e 3080 $m^2.day^{-1}$, with average of 540 $m^2.day^{-1}$ and median of 235 $m^2.day^{-1}$ (Almeida and Lourenço da Silva, 1990).

Recharge was originally estimated for the ARQ as 8.7×10^6 $m^3.year^{-1}$ (Almeida et al., 2000), based on an average rainfall of 550 mm and considering recharge rates of 50% for the jurassic and 15% to the miocene lithologies. Monteiro et al. (2007) presented a value of 5.4×10^6 $m^3.year^{-1}$ based on an average precipi-

tation of 593 mm/yr and corresponding to the infiltration of 23% of the rainfall on the areas of occurrence of formations with an intergranular porosity, and between 63% and 69% on the areas of occurrence of karst formations.

Groundwater abstraction for public supply extracted 3.3×10^6 m^3/year in 1993 (Almeida et al., 2000) and 8.43×10^6 m^3/year (~30% of the estimated average annual recharge) in 1999 (Hugman et al., 2013). After 1999, public water supply was mainly ensured by surface water. Almeida et al. (2000) estimated as 3.5×10^6 $m^3.year^{-1}$ (~12% of the estimated average annual recharge) the water extractions for irrigation in 1979.

Recently numerical flow models were applied to quantify the SGD and the impact of changes in groundwater use (Hugman et al., 2013; Monteiro et al., 2007). These authors used the ARQ boundaries defined by Almeida et al. (2000) and shown in Figure 1.

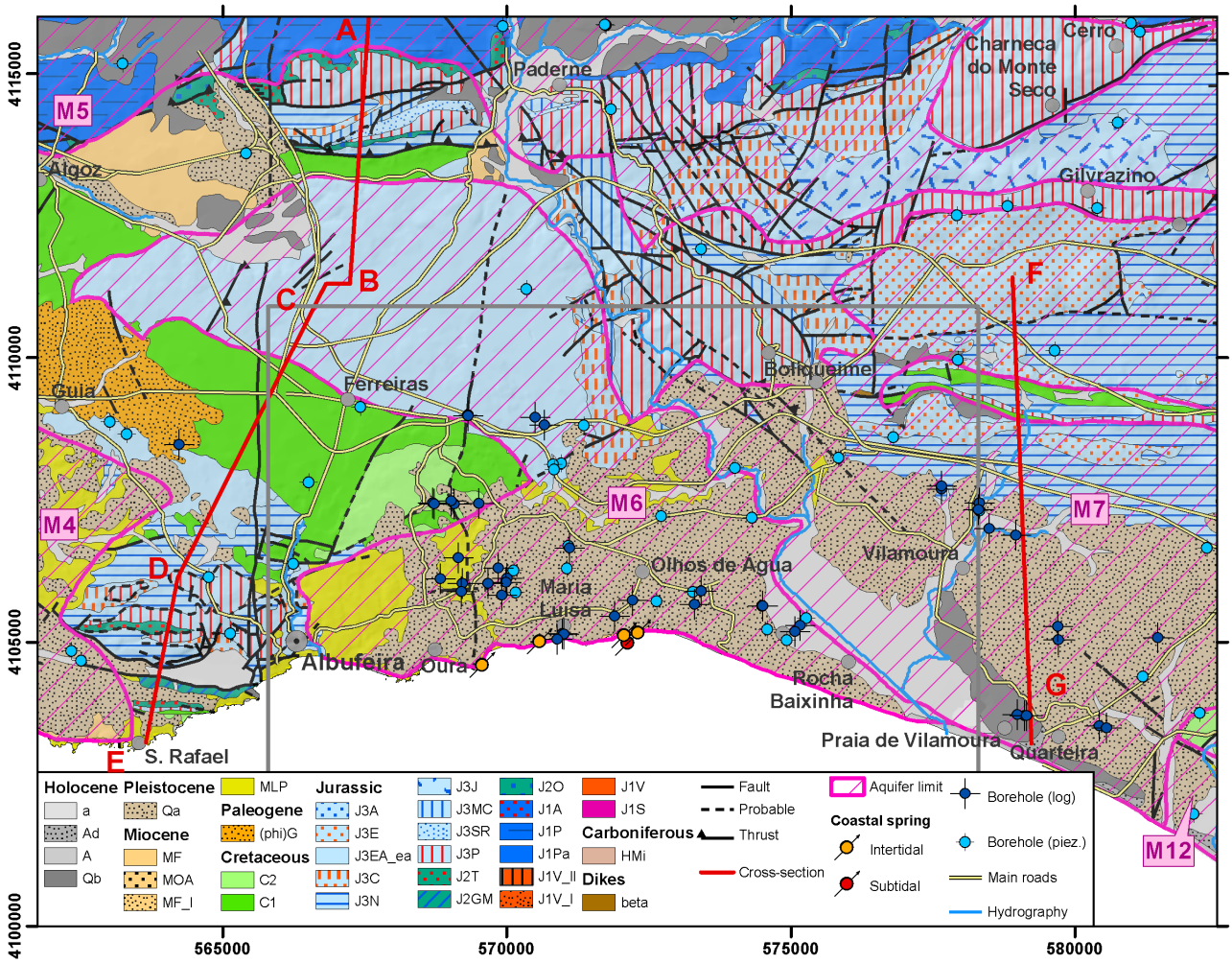

Figure 1 - Geological map of the study area (adapted from Manuppella, 1992). Grey rectangle indicates the position of Figure 5. Coordinates system (also in next figures): UTM N29, WGS 84. Aquifer systems abbreviations (Almeida et al., 2000): M4 Ferragudo - Albufeira; M5 Querença - Silves; M6 Albufeira - Ribeira de Quarteira; M7 Quarteira; M10 São João da Venda - Quelfes; M12 Campina de Faro.

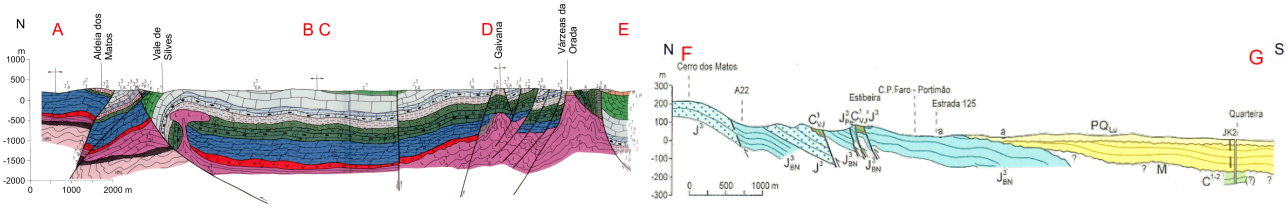

Figure 2 – Geological cross-sections (left: Manuppella (1992); right: Manuppella et al. (2007)), location in Figure 1.

Table 1 – Lithostratigraphy and hydrostratigraphy of the study area (adapted from Almeida and Lourenço da Silva, 1990; Almeida et al., 2000; Manuppella, 1992; Pais et al., 2000).

Epoch	Age	Symb.	Formation		Lithology	Thickness	Main lithology	Hydrostratigraphy
Pleistocene?	?	Qa	Faro-Quarteira sands		Clayey sandstones with pebbles intercalations	10-30m	Detritic	Aquitard
Pliocene	Piazencian	MOA	Olhos de Água sands		Feldspathic sands, pebbles			
Miocene	Burdigalian-Serravian	MLP	Lagos-Portimão Formation		Biocalcarenites, yellow or pink, sandy limestones and sandstones	30-85m	Limestone	Aquifer
Lower Cretaceous	Aptian	C2	Limestones and marls with *Palorbitolina lenticularis*		Massive limestones and marls, brownish	10m	Marl and limestone	Aquitard
	Barremian	C2	Marls with *Choffatella decipiens*		Marls, sandstones, marly limestones and dolomites	25m		
	Berriasian	C1	Sobral sandstones		Sandstone with quartz gravels, pebbles and pelites, redish to purple	50m	Detritic	
Upper Jurassic	Titonian	J3A	Limestones with *A. lusitanica*		Massive limestones whitish with calciclastic intercalations	650m	Limestone and dolomite	Aquifer
	Kimmeridgian	J3_EA	Escarpão limestones	Transition limestones	Massive limestones whitish with clayey intercalations			
		J3E		Limestones with *V. striata* and *C. jurassica*	Massive limestones, whitish to grey			
		J3_EA		Limestones with *A. jaccardi*	Massive limestones, whitish, with Nerineas and oncolithes			
		J3N	Sta Bárbara de Nexe dolomitic limestones and dolomites		Dolomitic limestones and dolomites, pinkish or yellowish			
		J3C	Cerro da Cabeça biolimestones		Massive limestones with recif fossiles			
	Oxfordian-Lower Kimmeridgian	J3P	Peral marls and limestones		Alternance of sandy and or marly limestones, massive, yellow and grey, with blue/grey marls	80-100m	Marl and marly limestone	Aquiclude

2.2 Hydrogeophysics

As there are still uncertainties in the ARQ conceptual model, we applied hydrogeophysic methods to contribute to review and hypothetically upgrade the ARQ geometry, boundary and structure, including hydraulic relationships between the hydrogeological formations. The geophysical methods we used consisted on: (i) 1D time domain electromagnetics (TDEM); (ii) quasi-2D frequency domain electromagnetics (FDEM); (iii) 2D continuous vertical electrical soundings (CVES).

2.2.1 Time domain electromagnetics

We used a TEM-FAST 48 from Applied Electromagnetic Research (AEMR) company with square loop of 25 or 50 m side (1 turn) in coincident loop configuration with an input current of 24 V and 4 A. A minimum of 3 curves at each site was acquired to confirm the repeatability of the measurement and the absence of EM noise induced by galvanic and/or capacitive coupling (Danielsen et al., 2003). The data were inverted using the software TEM-RES v7 from AEMR. When necessary, noisy data were firstly removed. Afterwards, using automatic inversion and trial and error method, a theoretical curve was fitted on observed data. The criterion of selection of the final solution was based on the minimum number of layers for the same quality of fitting, as well as hydrogeological knowledge of the area completed by local observation or borehole logs and coherency with the other geophysical methods.

2.2.2 Frequency domain electromagnetics

We used an EM-34 from Geonics instrument. The Geonics EM-34 device allows conducting a fast mapping of the lateral geolectrical variability of the subsurface, being particularly suitable to map saline intrusions (McNeill, 1980). It is composed by a transmitter coil Tx and a receiver coil Rx located at a predefined distance from Tx. This method is extremely easy and fast to use in the field and requires a minimum of 2 operators, one at each coil. During the data acquisition operations, special care must be taken regarding possible electrical interferences (industrial noise, transport lines of 50/60 Hz or even atmospheric noise).

At each measurement point, we obtained a vertical sounding with the 6 possible configurations, i.e. horizontal and vertical dipoles with cable spacings of 10, 20 and 40 m, allowing to reach investigation depths between 7.5 and 60.0 m. With several soundings along a line and applying a proper inversion algorithm, it is possible to obtain a subsurface 2D profile of the electrical resistivity variation. In this study, geoelectrical 2D modeling was conducted using the algorithm EM34-2D, which applies a 1D laterally constrained method (Santos, 2004). The obtained profiles allow to

visualize a model of the vertical distribution of electrical conductivities. The inverse problem is solved using a smooth inversion, where each 1D conductivity model, obtained beneath each measurement site, is constrained by its neighbors.

2.2.3 Geoelectrical

CVES were acquired in the field using an IRIS Syscal pro and an ABEM Terrameter SAS-4000. The former was configured with 4 cables 90 m long and a total of 72 electrodes, the latter with 4 cables 100m long and a total of 64 electrodes. We used several arrays such as schlumberger, wenner and dipole-dipole. We also used a Scintrex TSQ-3 equipment with 18 electrodes in dipole-dipole array with 1350 m length to detect large geological structures. Inversions were performed using RES2DINV v3.53, generally using model refinement and robust inversion. Bad datum points and points with RMSE > 60 or 80 % were removed from the inversion.

2.3 Auxiliary information

2.3.1 Boreholes logs

The lithological information of 45 borehole logs (Figure 1) obtained in drilling companies reports were collected from several institutions' archives (Laboratório Nacional de Energia e Geologia – LNEG, Agência de Região Hidrográfica do Algarve - ARHA). The boreholes logs were interpreted to associate the described lithologies to the geological and hydrogeological formations referred in Table 1. This information was used to support the interpretation of the hydrogeophysics results.

2.3.2 Hydraulic heads and regional static piezometric surface

The objective of the piezometric analysis was not to obtain a regional piezometric surface *per se* but to highlight high and low hydraulic gradient areas to detect hydraulic barriers, preferential flow zones and other relevant hydrogeological features. The retrieval of a reliable static piezometric surface requires the availability of a good spatial distribution of boreholes and measurements made during a short period with same hydrological conditions. Although a high boreholes density was available in the ARQ CA, most of them are under exploration and equipped with pumps, which does not allow us to use a dipper (high risk of blocking the dipper's tape with the pump's cables). Hydraulic heads measurements were only possible in 22 boreholes equipped with dip tube and belonging to the Albufeira municipality (CMA). Hydraulic heads were also available from 69 boreholes belonging to the monitoring program of the Portuguese Water Institute (INAG, snirh.pt). We thus compiled the historical data from INAG and CMA archives to obtain the final hydraulic heads dataset composed by records from March 1978 to December 2013 of 91 boreholes. Note that the piezometric measurements in the CMA boreholes were made after being deactivated, i.e. from 2001. They thus correspond to the static piezometric level.

The maximum number of concomitant hydraulic heads was only 29 (8 of them inside the ARQ area). We thus elaborated the static piezometric surface using the lowest hydraulic head at each of the 91 boreholes to retrieve the regional piezometric surface. We assumed that the lowest hydraulic head is the most reliable value in absence of pumping because the recession part of the well hydrograph follows an exponential decay that is asymptotic towards the local base level (Dingman, 2002). After selecting the lowest hydraulic heads, we interpolated it using simple kriging.

2.3.3 Analytical models of the freshwater–saltwater interface

The Dupuit-Ghijben-Herzberg model (Dingman, 2002; Fetter, 2001) allow to compute the position of the FSWI under the assumptions of sharp interface and 1D flow in a homogeneous unconfined coastal aquifer, as following:

$$z = \sqrt{2xq_tG/K} \quad (1)$$

where z is the depth of the interface below sea level, x is the distance inland from the coast, q_t is the groundwater discharge at the coastline per unit width, G is equal to $\rho_w/(\rho_s - \rho_w) \simeq 40$, with ρ_w and ρ_s density of fresh and salt water respectively, and K is hydraulic conductivity.

However in this model the FSWI intercepts the water table at the coastline, which doesn't correspond to the real situation. The Glover model (Dingman, 2002; Fetter, 2001) considers an outflow face of freshwater discharge into the sea as following:

$$Z = \sqrt{2xq_tG/K + {q_t}^2G^2/K^2} \quad (2)$$

$$x_0 = -q_tG/2K \quad (3)$$

$$h = \sqrt{2xq_t/GK} \quad (4)$$

where x_0 is the width of the outflow face and h is the height of the water table above sea level.

3 RESULTS

3.1 Regional static piezometric surface

The regional static piezometric surface obtained by interpolation of the lowest hydraulic heads of 91 boreholes is shown in Figure 3. The depth of most of these boreholes is unknown. However, from the analysis of the borehole with logs (Figure 1), we observed that boreholes screen the shallowest aquifer and are connected with only one aquifer.

The regional static piezometric surface (Figure 3) highlighted the limits of the ARQ aquifer and its compartments. It confirms the north limit that is marked by a clear contrast between high hydraulic heads in ARQ and low hydraulic heads in Querença-Silves aquifer (respectively M5 and M6 aquifers in Figure 1 and Figure 3). The east boundary is also confirmed since the computed equipotential lines are parallel to the Quarteira river when boreholes are available at the both side of the river. The west boundary is also strongly marked by a strong contrast of hydraulic heads between ARQ and Ferragudo – Albufeira aquifer (M4). A clear distinction can also be made between the hydraulic heads in the Jurassic and the Miocenic formations inside the ARQ, showing clearly that these two aquifers are not fully hydraulically connected. The general flow direction is towards South in the miocenic aquifer while it is south and SE in the Jurassic aquifer. Note that the increase of hydraulic heads between Oura and Albufeira, i.e. in an area of miocenic outcrops, seems to be an artifact because no boreholes are available in this area. At north of this sector, the hydraulic heads in the cretaceous outcrops are in continuity with the one of the Jurassic formations. This fact is supported by the hydraulic heads of 3 boreholes located in the cretaceous outcrops. Although the depth of these boreholes is unknown, it is very probable that they are implemented in the Jurassic aquifer, which means that the jurassic aquifer extend towards the sea below the cretaceous and the miocenic formations.

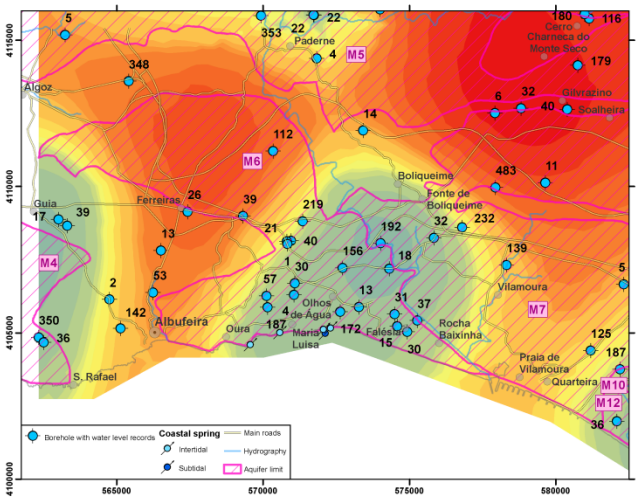

Figure 3 – Regional static piezometric surface retrieved using the lowest hydraulic head of each borehole (black label next to the borehole symbol indicates the number of values). Red colors indicate high hydraulic heads, blue colors indicate low hydraulic heads.

3.2 Analytical models

The analytical models were applied using the collected information of the aquifer system, i.e. hydraulic conductivity of 1 and 5 m.d^{-1} (minimum and intermediate values) and recharge of 23800 m^3.d^{-1}. We tested the impact of low and high recharge by applying a multiplier factor *n* with value of 0.5, 1.0 and 2.0.

The application of the analytical models (Figure 4) shows that:

- the width of the outflow interface (x_0) varies from 119 m to 6 m, while the depth of the FSWI at coast line varies between 238.0 and 11.9 m. Subtidal springs were indeed observed during diving at ~120 m from the coast (Figure 1).
- high recharge and low K, as they increase the hydraulic gradient, provokes wider outflow face as well as deeper and steeper FSWI.
- the interface inclination is smooth for the intermediate case (i.e. K = 5, n = 1). At 200 m from the coast line towards inland, the FSWI is only 100 m deep. With the lowest recharge (n = 0.2), the depth is 100 m at 400 m of the coast and 150 m at 1 km. Note that with the maximum K (100 m.day^{-1}), the Glover model indicate much shallower FSWI (plot not shown here).

Although these facts indicate a high risk of upconing since boreholes in the ARQ area reach the depth of the modelled FSWI, the real hydrogeological settings (high heterogeneities with spatially variable K, karstification and confining units) are much more complex that the one assumed in the model. Nevertheless, the Glover model gives a valuable information about the FSWI position and its dynamic.

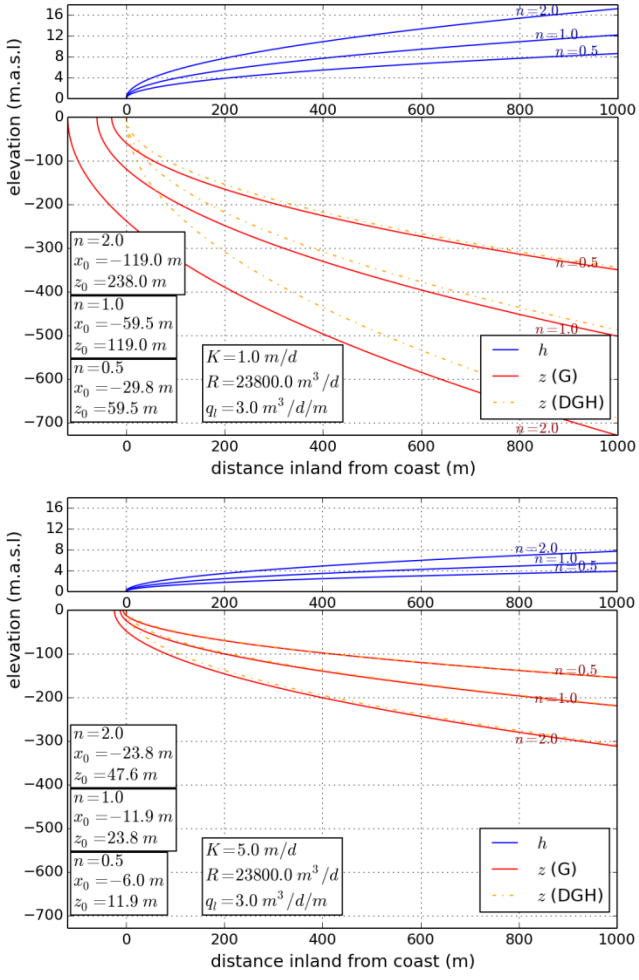

Figure 4 – Analytical model of the freshwater-saltwater interface (note the difference of vertical scale above and below sea water level). G: Glover model;GDH: Dupuit-Ghyben-Herzberg model; z_0: depth of the interface at the coast line; n: recharge multiplier. See text for other abbreviations.

3.3 Hydrogeophysics

Based on the previous analysis, we detected the following questions in relation to the current ARQ limits and structure:

- Is the cretaceous present between the miocenic and jurassic aquifers?
- Is the cretaceous stripe outcropping between the jurassic and the miocenic in the central west part of the aquifer, i.e. between Ferreiras and Albufeira, a hydraulic barrier or just aquitard semi-confining the jurassic aquifer?
- What is the shape and position of the FWSI, and its spatial variation along the coast?
- How can we explain the concentration of the SGD, namely at Olhos de Água?
- How deep is the piezometric surface between Oura and Albufeira?

These questions are relevant to setup a variable-density groundwater flow numerical model and may have strong implications in the computing of its resultant water balance. To check the hydrostratigraphy, hydraulic relationships, depth of the water table and detection of the FSWI, we performed hydrogeophysical surveys between January 2013 and December 2013 composed by 18 TDEM soundings, 3 FDEM profiles, 11 CVES profiles organized in 5 transects transversal and longitudinal to the main groundwater flow (A, B, C, D and E in Figure 5). The methods were used to detect the position and slope of the FSWI by surveys on the coastal cliffs (TDEM, CVES), along the beach (CVES) and in profiles perpendicular to the coast (FDEM). TDEM and CVES were also used to detect the water bearings formations, as well as the cretaceous aquitard below the miocenic aquifer. For this last purpose, 2 CVES were realized using the Scintrex equipment to detect in depth the geological contact. CVES method was also performed to detect karstic structure and fresh water springs on the beach due to its relatively high-resolution and cross-sectional characteristics. Note that the high urban development in the study area constrained the use of hydrogeophysics (lack of extension to deploy CVES cables, electromagnetic noise limiting the use of TDEM and FDEM) in areas that we considered important.

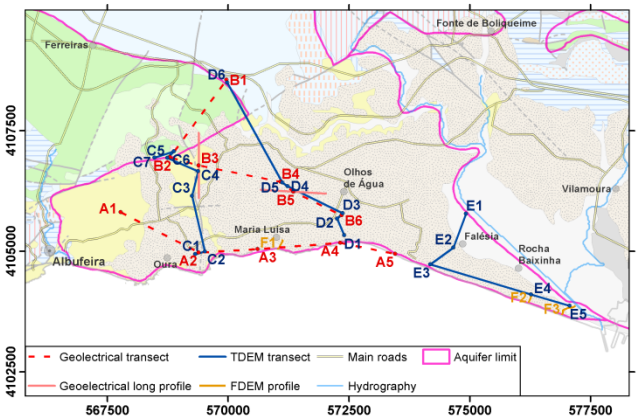

Figure 5 – Localization of the hydrogeophysics surveys.

The CVES longitudinal transect A1 to A5 (Figure 6) shows at A1 the water table at ~10 m above sea level (m.a.s.l.). Above, it corresponds to unsaturated miocenic aquifer with resistivity between 75 and 200 ohm.m. The saturated zone shows a ~15 m thick layer of resistivity ~50 ohm.m above a layer of low resistivity (10 ohm.m). As there is no clayey layer in the Lagos-Portimão formation, we interpreted this result as fresh water above brackish-salt water. The saltwater is very shallow, i.e. -10 m.a.s.l., at ~1300 m from the coast. For comparison, the Glover model with highest K = 100 m.d^{-1} (plot not shown here) indicates the FWSI at ~-50 m.a.s.l. at this coastline distance. The shallow salt water observed in A1 CVES can be explained by two processes: (i) upconing; (ii) diapirism. Independently of the source of the salt water, the salinization is probably provoked by the large volumes of groundwater pumped by private boreholes belonging to the many Albufeira touristic installations (hotels and resorts). Indeed,

the monitoring of the groundwater electrical conductivity in these private boreholes shows seasonal variations from 100 to 1000 µS.cm^{-1} (data gently provided by the Albufeira municipality).

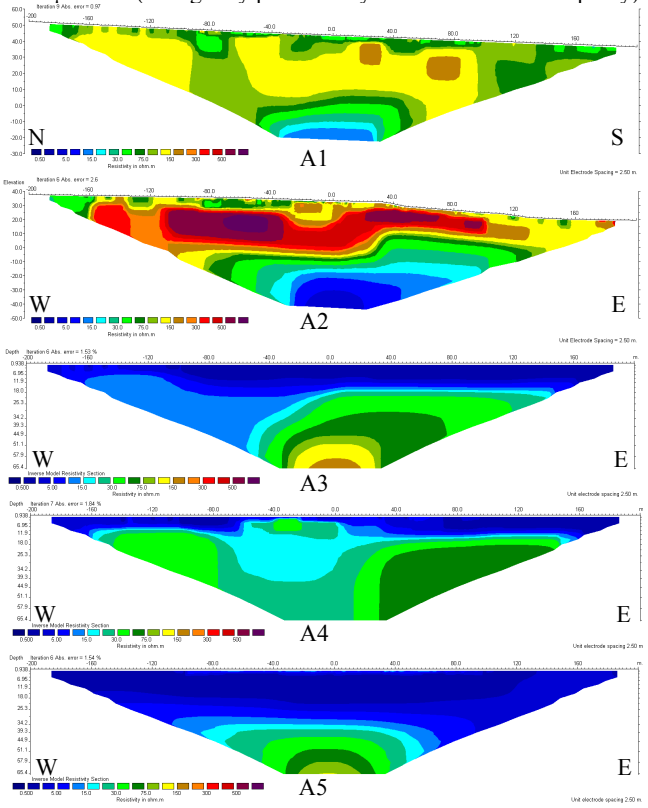

Figure 6 – Longitudinal transect of geolectrical profiles (see location in Figure 5).

At site A2, located at ~400 m from the coast, the highest resistive layer (100-600 ohm.m) corresponds to the plio-quaternary formations. Below, the ~50 ohm.m layer corresponds to saturated miocenic formations. As the plio-quaternary and the miocenic formations are outcropping on the nearby cliffs, we measure the elevation of this geological contact using a differential GPS. We found a very good agreement with the elevation obtained with the CVES. Moreover, the contact between the plio-quaternary and the miocenic formations shows an uplift on the right section of the CVES, i.e between abscissa 30 and 180 m. This uplift corresponds to the expression of the NS geological fault visible in Figure 1. The fact that the top of the saturated miocenic layer follows this uplift indicates that miocenic aquifer is confined by the plio-quaternary formations. The deepest layer is characterized by low resistivity (< 10 ohm.m) of saltwater, below a flat surface at -10 m.a.s.l. Together with the presence of a intertidal freshwater spring located W of the fault (Figure 1), these settings are in agreement with the Glover model. West of the fault, the freshwater layer is very thin (~10 m), which constitute a high risk of upconing. Indeed, the groundwater electrical conductivity measured from a private borehole located at the W edge of the CVES was between 2000 and 2500 µS/cm.

The CVES A3 to A5 present similar settings: low resistive layer (> 10 ohm.m) above a layer of resistivity ~20-100 ohm.m. The first layer corresponds to seawater in beach sands while the second to fresh groundwater in miocenic formations. This configuration is explained by coastal fringe processes, such as tidal dynamic and upper seawater recirculation zone (Werner et al., 2013). Karsts features, expressed by blocks of slightly different resistivity, are also visible on CVES A3 and A4. An intertidal freshwater discharge is visible at A4 between abscissa -60 and 0. Finally, the deepening of the top of the miocenic formation towards east is clearly visible from A4 to A5. However the plio-quaternary was expected between the sand beach and miocenic expression, but either it is not present or its resistive signature is similar to the sand beach, which is probable due to the presence of saturated clayey lithologies.

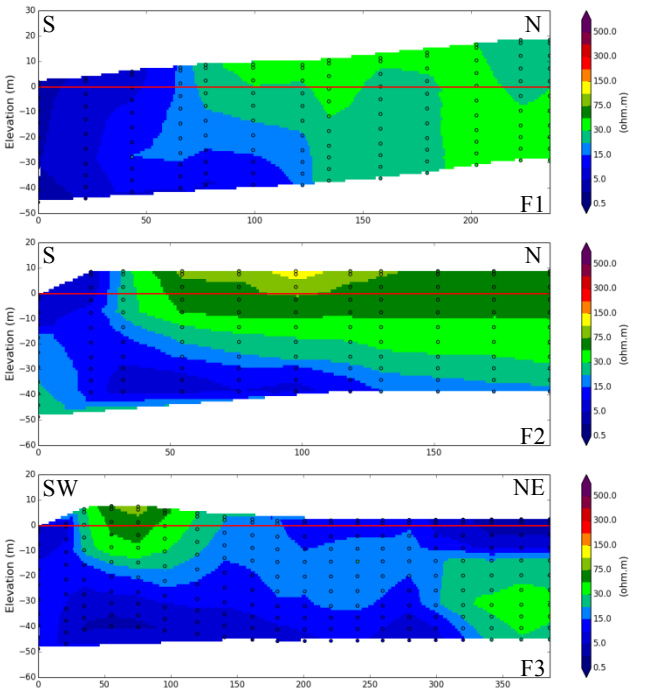

Figure 7 – FDEM profiles. (see location in Figure 5). These profiles show steep (F1) and smooth (F2 and F3) inclined freshwater-saltwater interface. All profiles were starting from the beach, located at South.

The FDEM profiles of Figure 7 show at S formations with seawater, characterized by low resistivity (<15 ohm.m) and at N freshwater saturated formations with resistivity of ~30-50 ohm.m. At F1 the freshwater formations correspond to miocenic aquifer while at F2 and F3 they correspond to alluvium, dune and beach sands. The slope of the FSWI is clearly imaged, showing a steep inclination at F1 while at F2 and F3, located in the most oriental part of the AQR, the inclination is smooth. This geometry was expected and is in agreement with the Glover model, since the hydraulic heads are quite low in the oriental sector. Below the Quarteira river, at NE of the F3 profile, the ~30-50 ohm.m resistivite layer seems to indicate fresh groundwater. Above, the low resistivity layer indicates saltwater intrusion from the Quarteira stream inside the alluvium aquifer. This profile exemplifies the complex relationships between the Quarteira river and the aquifers, with a temporal variation of influent and effluent characteristics at the same location.

On transect B (Figure 8), B1 makes visible the contact diving towards S between jurassic and cretaceous formations (respectively resistivities of ~100-200 ohm.m and ~10-75 ohm.m). The cretaceous formations have similar signature than saturated miocenic observed previously, although they show a larger range due to the presence of low resistivie clayey/marly layers. At B2, exclusively made in cretaceous formations, a fault diving towards NE seems to separate a blocks of lower resistivity at S of 100 m abscissa. The long CVES B3, east of B2, identified clearly a vertical anisotropy between abscissa 525 and 565 m with resistivity ~150-200 ohm.m. The interpretation is difficult since the plio-quaternary is covering the underlain geological formations. The water table was measured at 5 m.a.s.l in an abandoned borehole south of the B2 CVES. However, due to the coarse resolution, it is uncertain to recognize the water table on the B2 CVES. At B4, the interpretation is supported by a municipality's borehole 187 m deep. The surficial ~15 m thick, resistive layer (~100-200 ohm.m) corresponds to plio-quaternary formations. Below, the miocenic formations show resistivity between 30 and 100 ohm.m. The water level measured in the borehole was -5 m.a.s.l. but is not visible in the CVES profile, although a slight resistivity increase of resistivity is observed below this depth. The long dipole-dipole B5 CVES represents better the geological layering despite an unidentified structure with resistivity of 100-200 ohm.m in the middle of the profile. The borehole logs shows, below a plio-quaternary layer 26 m thick,

typical miocenic lithology from 16 to -54 m.a.s.l., that we relate to the B5 horizontal stripe between 0 and -80 m, and marly limestones between -54 and -97 m.a.s.l., probably cretaceous, that we related to the low resistivity below -80 m. Between 97 and 146 (bottom of the borehole), the log described grey and reddish hard limestones that may correspond to the jurassic formations. The differences in elevation between the borehole and the inverted resistivity profiles are due to the coarse resolution of the geoelectrical acquisition array (75 m inter-electrode distance). Finally, B6, located ~1km to ~600 m from the coast and A4, show ~20 m of plio-quaternary (resistivity of 150-700 ohm.m) on top of miocenic formations (resistivity of 50-100 ohm.m). As in A2, the miocenic is probably confined.

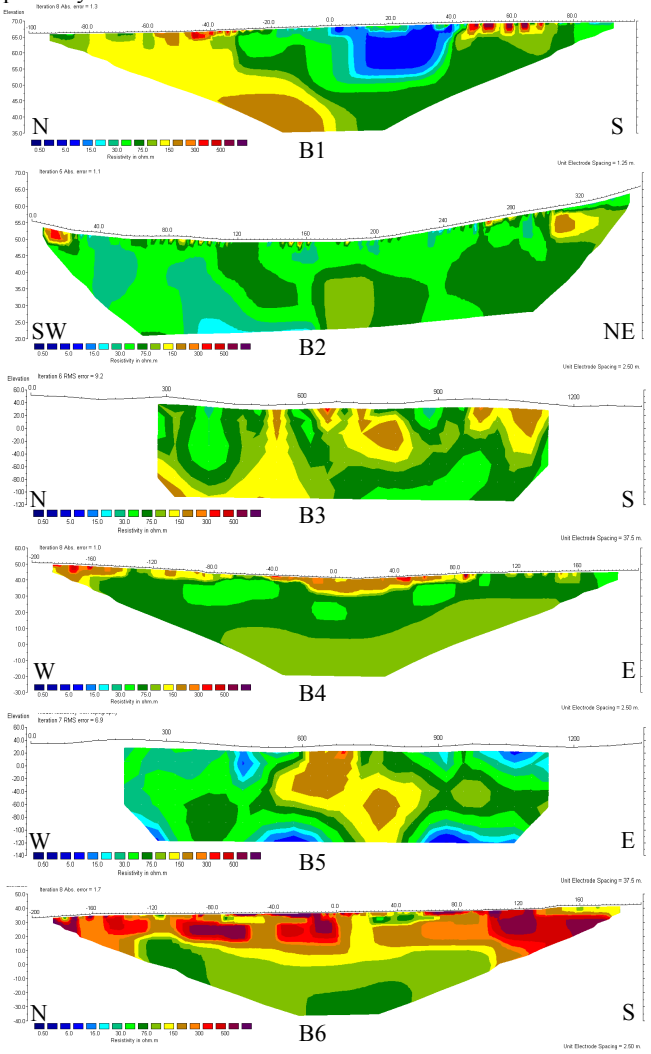

Figure 8 –Transversal transect of geoelectrical profiles (see location in Figure 5). Note that profiles B3 and B5 were ~1400 m long, reaching a depth of ~120 m, while the other ones were ~400 m long or less.

The TDEM C2, D1, D2, D3, close to coast shore, show low resistivity at their last layer, which depth increase from coast to inland. This contrast seems to indicate the FSWI. Above, the layer with resistivity between 20 and 75 ohm.m indicates the miocenic aquifer, in agreement with the CVES. The upper resistive layer (> 150 ohm.m) indicates the plio-quaternary unit. More inland, one can identify a low resistivity layer at C3, C4 and D5 (distance of ~2000 m from the coast) as well as in C78 (> 3000 m from the coast). This low resistivity at a far distance from the coast, as observed in CVES profile A1, may correspond to groundwater salinization due to upconing and/or diapirism. Finally, the E profile indicates similar information as CVES A3 to A5. The low resistivity observed at E1 (~15-20 ohm.m) seems to indicate that the Quarteira river is influent in the alluvium aquifer and provokes groundwater salinization. E2 gives information that may help to interpret the CVES A5. Below a high resistive layer (> 500 ohm.m) corresponding to unsaturated plio-quaternary observed on the cliff, a thin layer appears with very low resistivity, being above a layer with resistivity of ~30-50 ohm.m. The latter corresponds to fresh groundwater in the buried, confined miocenic aquifer, while the latter corresponds to saturated plio-quaternary that, due to its high clay content, shows very low resistivity similar to the the resistivity of seawater saturated beach sand.

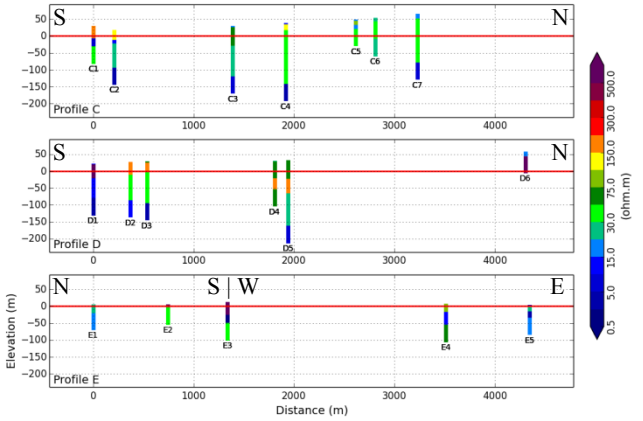

Figure 9 – TDEM transects (see location in Figure 5). Deepest layer arbitrarily set to 50 m thick.

4 DISCUSSION

4.1 Geolectrical model

The resistivity ranges of the hydrogeological formations of the study area are presented in Table 2. It was observed a very good agreement between the 3 geophysics technics. TDEM is more expedite to perform in the field, although more sensitive to EM noise, while CVES gave a very good overview of the spatial relationship between the hydrogeological formations.

Table 2 – Geoelectrical range of the formations. PQ: plio-quaternary; Mio: miocenic; Cret.: cretaceous; Jur.: jurassic; FW: freshwater; SW: saltwater; BW: brackish water.

Layer	Resistivity range (ohm.m)	Profile
Sand beach (SW)	<10	A3-5
PQ unsat.	100-700	A2, B4, B6, A2
PQ sat.	10-15	A3
Mio unsat.	75-200	A1
Mio. sat. (FW)	20-100	A-5, B4, B6
Mio. sat. (S/BW)	< 10	A1-2
Cret.	10-100	B1, B2, B5
Jur. unsat.	100-200	B1

Our results are in agreement with previous geoelectrical surveys (unpublished work from the Amsterdam Free University). For instance, one of this study (Elsendoorn et al., 1982) presents a NS geoelectrical profile made with 5 vertical electrical soundings (VES), located N to Olhos de Água and ~4 km long, in which the plio-quaternary has resistivity ~270 ohm.m, the saturated Miocene ~110 ohm.m, the upper cretaceous (C2 in Table 1) ~25 ohm.m, and the cretaceous C1 60-100 ohm.m. The cross section presents a subtabular plio-quaternary above miocenic and cretaceous formations diving towards S. The marly cretaceous formations were also identified below the miocenic ones by other authors in the Quarteira region (Carvalho et al., 2012; Carvalho et al., 2006; Geirnaert et al., 1982).

The hydrogeophysical interpretation is still ambiguous due to two main reasons: (i) too shallow depth of penetration; (ii) overlap of resistivity ranges of geological formations. The use of a complementary method, such as seismic (Carvalho et al., 2012) or magnetic resonance soundings MRS (Legchenko et al., 2009; Vouillamoz et al., 2012), which targets to other material properties (seismic wave propagation and presence of hydrogen, respectively), may be of great use to solve the two enunciated limitations.

4.2 Contribution to the ARQ HCM

The presence of the cretaceous between the miocenic and the jurassic formations seems to be confirmed by the geophysics results of this study and the previously cited studies. As the cretaceous formations behave as an aquitard, it explains the hydraulic heads difference between miocenic and jurassic aquifers. It is this probable that the jurassic aquifer recharge the miocenic aquifer through the cretaceous aquitard. Such hypothesis could be tested using numerical groundwater flow model. To do so, we propose to extend the current ARQ west boundary towards the Albufeira NS fault.

We also detected several accidents affecting the miocenic and cretaceous formations (CVES B1, B3, B5?) that were not identified in the geological map of Figure 1 simply because the plio-quaternary formation are covering the area.. These faults may have a strong influence in the hydrogeology and hydrochemistry of the groundwater, namely in groundwater salinization by diapir ascension. On other hand, seawater intrusion can occur very far from the coast. For instance, de Montety et al. (2008) showed than in a confined aquifer of the Camargue region (France), the proportion of saltwater reaches 98% in the aquifer at 8 km from the coast. Several CA in the mediterranean basin faces the problem of groundwater salinization, provoked in many cases by several sources (Mongelli et al., 2013; Trabelsi et al., 2012). To distinguish diapiric and sea origins, extensive hydrogeochemical survey must be done to complement previous work (Bronzini, 2011).

The concentration of the inter- and subtidal freshwater springs at Olhos de Água can be explained by the geological settings. Indeed, the submerse miocenic formations are confined by plio-quaternary at east of Olhos de Água. No SGD were detected in this area by off-shore surveys of electrical conductivity, temperature and depth in the sea, while between Albufeira and Olhos de Água there is clear indices of SGD (Sousa et al., 2013). With a groundwater flow towards S and SE, the groundwater is trapped in the submersed miocenic formations and the discharge must occur at Olhos de Água. Thesehypotheses also means that below the off-shore miocenic aquifer may store large groundwater resource, as it was recognized in recently in several world CA (Post et al., 2013). Once again, variable-density groundwater flow numerical model may be crucial to test such hypothesis. Such model would have to integrate the off-shore geology, which requires costly off-shore geophysics surveys and interpretation. On other hand, it would be very important to optimize the monitoring network, with at least one piezometer in each sector of the aquifer (unconfined jurassic, unconfined miocenic, confined jurassic below cretaceous, confined jurassic below miocenic and cretaceous, confined miocenic below plio-quaternary). The spatio-temporal assessment of groundwater recharge using hydrometeorological network and distributed recharge model coupled with groundwater model (Francés et al., 2011) is also of crucial importance to constrain the groundwater model and reduce uncertainties.

5 CONCLUSION

We performed a combination of TDEM, FDEM and CVES surveys to clarify some issues related with conceptual modelling of the ARQ CA. Our results are in agreement with other geophysical study in surrounding areas. The geophysical methods were effective in the detection of the position of the FSWI and allowed redefining the boundaries and 3D structure of the aquifer, as well explaining the SGD location. Such insights permit to elaborate hypothesis that can be tested by the implementation of numerical groundwater flow models. The interchange of information between numerical modelling and hydrogeophysics model is an iterative work towards less uncertain groundwater model and water balance, which could allow to improve the water management in CA and minimize groundwater salinization risk.

6 ACKNOWLEDGEMENT

This study was supported the project “FREEZE – Submarine Fresh Water Discharges: Characterization and Evaluation Study on their Impact on the Algarve Coastal Ecosystems” (PTDC/MAR/102030/2008), founded by Fundação para a Ciência e a Tecnologia (FCT). We thank the Câmara Municipal de Albufeira for the access to the municipality boreholes, Edite Reis (ARHA) to provide the borehole data, Teresa Cunha (LNEG) to provide the digital geological cartography and Manuel Silva (LNEG) for the geoelectrical field work.

7 REFERENCES

Almeida, C.A.C., Lourenço da Silva, M., 1990. Hidrogeologia do Miocénico entre Albufeira e Ribeira de Quarteira. Geolis, IV(1 e 2): 16.

Almeida, C.A.C., Mendonça, J.J.L., Jesus, M.R., Gomes, A.J., 2000. Sistemas aquíferos de Portugal continental, Lisbon.

Auken, E. et al., 2010. The use of airborne electromagnetic for efficient mapping of salt water intrusion and outflow to the sea. The use of airborne electromagnetic for efficient mapping of salt water intrusion and outflow to the sea.

Aunay, B. et al., Hydro-socio-economic implications for water management strategies: the case of Roussillon coastal aquifer, Colloque international sur la gestion des grands aquifères, 150è anniversaire de la loi de Darcy, 50ème anniversaire de l'AIH (Association Internationale des Hydrogéologues), pp. 9 p.

Aunay, B. et al., 2007. A multidisciplinary approach for assessing the risk of seawater intrusion in coastal aquifers: The case of the Roussillon Basin (France). Aquifer Systems Management: Darcy’s Legacy in a World of Impending Water Shortage: Selected Papers on Hydrogeology 10: 459.

Bakker, M., Schaars, F., 2005. TheSea Water Intrusion (SWI) package manual Part I: Theory user manual and example, version 1.2, www.modflowswi.googlecode.com.

Barazzuoli, P., Nocchi, M., Rigati, R., Salleolini, M., 2008. A conceptual and numerical model for groundwater management: a case study on a coastal aquifer in southern Tuscany, Italy. Hydrogeology Journal, 16(8): 1557-1576.

Bronzini, S., 2011. Etude hydrogéologique de la zone d’Albufeira (Algarve, Portugal) et analyse des mécanismes de salinisation des eaux souterraines. Master en hydrogéologie et géothermie, spécialisation en hydrogéologie Thesis, Université de Neuchâtel, Switzerland, 83 pp.

Carrara, G., 2012. Submarine fresh groundwater discharge investigation: a multidisciplinary approach, VII Simpósio sobre a Margem Ibérica Atlântica, Lisbon.

Carvalho, J., Ramalho, E., Dias, R., Pinto, C., Ressurreição, R., 2012. A Geophysical Study of the Carcavai Fault Zone, Portugal. Pure and Applied Geophysics, 169(1-2): 183-200.

Carvalho, J., Torres, L., Rocha, R., Dias, R., Mendes-Victor, L., 2006. A geophysical study of the S. Marcos–Quarteira fault, Portugal. Journal of Applied Geophysics, 60(2): 153-164.

Creel, L., 2003. Ripple effects: population and coastal regions, Making the link. Population Reference Bureau.

Custodio, E., 2010. Coastal aquifers of Europe: an overview. Hydrogeology Journal, 18(1): 269-280.

Danielsen, J.E., Auken, E., Jørgensen, F., Søndergaard, V., Sørensen, K.I., 2003. The application of the transient electromagnetic method in hydrogeophysical surveys. Journal of Applied Geophysics, 53(4): 181-198.

de Montety, V. et al., 2008. Origin of groundwater salinity and hydrogeochemical processes in a confined coastal aquifer: Case of the Rhône delta (Southern France). Applied Geochemistry, 23(8): 2337-2349.

Dingman, S.L., 2002. Physical hydrology. Prentice Hall, Upper Saddle River, 646 pp.

Dörfliger, N., 2013. Entre terre et mer, les eaux souterraines du littoral. Géosciences (BRGM), 17: 74-81.

Elsendoorn, B., Hoogeveen, H., Vuyck, P., 1982. Geo-electrisch onderzoek van de Miocene aquifer tussen Olhos de Agua en Quarteira, Algarve (Portugal). VU University, Faculty of Earth and Life Sciences, Amsterdam.

Encarnação, J. et al., 2013. The influence of submarine groundwater discharges on subtidal meiofauna assemblages in south Portugal (Algarve). Estuarine, Coastal and Shelf Science, 130(0): 202-208.

Fetter, C.W., 2001. Applied Hydrogeology. Prentice Hall PTR, 598 pp.

Fleury, P., Bakalowicz, M., de Marsily, G., 2007. Submarine springs and coastal karst aquifers: A review. Journal of Hydrology, 339(1–2): 79-92.

Francés, A.P., Reyes-Acosta, J.L., Balugani, E., van der Tol, C., Lubczynski, M.W., 2011. Towards an improved assessment of the water balance at the catchment scale : a coupled model approach. In: J.M. Fernández, N.S. Martin (Ed.), Estudios en la zona no saturada del suelo : volumen X : ZNS11 proceedings, 19-21 October, Salamanca, Spain, pp. 321-326.

Geirnaert, W., van Beeres, P.H., de Vries, J.J., Hoogeveen, H., 1982. Hidrogeologic studies in the East Algarve, Portugal. Part I: Geo-electric survey of the miocene aquifer between Quarteira and Olhao, Algarve, Portugal., III Semana de Hidrogeologia, 10 - 14 May, Lisbon, Portugal, pp. 2-22.

Henderson, R. et al., 2010. Marine electrical resistivity imaging of submarine groundwater discharge: sensitivity analysis and application in Waquoit Bay, Massachusetts, USA. Hydrogeology Journal, 18(1): 173-185.

Hugman, R., Costa, L., Monteiro, J.P., Stigter, T., Nunes, L., 2013. Modelling the spatial and seasonal distribution of submarine groundwater discharge for different water use scenarios under epistemic uncertainty. Environmental Earth Sciences, Submitted (Special Issue: Sustainability & Water Resources).

Kok, A. et al., 2010. Using Ground based Geophysics and Airborne Transient Electromagnetic Measurements (SkyTEM) to map Salinity Distribution and Calibrate a Groundwater Model for the Island of Terschelling - The Netherlands.

Langevin, C.D., Thorne, D.T., Jr., Dausman, A.M., Sukop, M.C., Guo, W., 2007. SEAWAT Version 4: A Computer Program for Simulation of Multi-Species Solute and Heat Transport, U.S. Geological Survey Techniques and Methods Book 6, Chapter A22.

Legchenko, A., Ezersky, M., Camerlynck, C., Al-Zoubi, A., Chalikakis, K., 2009. Joint use of TEM and MRS methods in a complex geological setting. Comptes Rendus Geosciences, 341(10-11): 908-917.

Manuppella, G., 1992. Carta Geológica da Região do Algarve (1:100000). Serviços Geológicos de Portugal, Lisbon.

Manuppella, G., Ramalho, M., Telles Antunes, M., Pais, J., 2007. Sheet 53-A (Faro), Carta Geológica de Portugal (1:50 000). Laboratório Nacional Energia e Geologia, Lisbon.

Mongelli, G., Monni, S., Oggiano, G., Paternoster, M., Sinisi, R., 2013. Tracing groundwater salinization processes in coastal aquifers: a hydrogeochemical and isotopic approach in the Na-Cl brackish waters of northwestern Sardinia, Italy. Hydrol. Earth Syst. Sci., 17(7): 2917-2928.

Monteiro, J.P., Oliveira, M.M., Costa, J.P., 2007. Impact of the Replacement of Groundwater by Dam Waters in the Albufeira-Ribeira de Quarteira and Quarteira Coastal Aquifers, XXXV AIH Congress. Groundwater and Ecosystems, Lisbon, Portugal, pp. 10.

Oude Essink, G.H.P., 2001. Density Dependent Groundwater Flow - Salt water Intrusion and Heat Transport, Utrecht University.

Pais, J., Legoinha, P., Elderfield, H., Sousa, L., Estevens, M., 2000. The Neogene of Algarve (Portugal), 1º Congresso sobre o Cenozóico de Portugal. Ciências da Terra (UNL), 14, pp. 277-288.

Post, V., Abarca, E., 2010. Preface: Saltwater and freshwater interactions in coastal aquifers. Hydrogeology Journal, 18(1): 1-4.

Post, V.E.A., 2005. Fresh and saline groundwater interaction in coastal aquifers: Is our technology ready for the problems ahead? Hydrogeology Journal, 13(1): 120-123.

Post, V.E.A. et al., 2013. Offshore fresh groundwater reserves as a global phenomenon. Nature, 504(7478): 71-78.

Poulsen, S.E., Rasmussen, K.R., Christensen, N.B., Christensen, S., 2010. Evaluating the salinity distribution of a shallow coastal aquifer by vertical multielectrode profiling (Denmark). Hydrogeology Journal, 18(1): 161-171.

Presidência do Conselho de Ministros, 2009. Resolução do Conselho de Ministros n.º 82/2009 de 8 de Setembro de 2009, Diário da República, 1.ª série — N.º 174, pp. 6056-6088.

Santos, F.A.M., 2004. 1-D laterally constrained inversion of EM34 profiling data. Journal of Applied Geophysics, 56: 123-134.

Sousa, F. et al., 2013. Descargas de Águas Subterrâneas na região dos Olhos de Água, Algarve – alguns resultados das campanhas CTD, 8ª Assembleia Luso Espanhola de Geodesia e Geofísica, Évora (Portugal).

Trabelsi, R., Abid, K., Zouari, K., Yahyaoui, H., 2012. Groundwater salinization processes in shallow coastal aquifer of Djeffara plain of Medenine, Southeastern Tunisia. Environmental Earth Sciences, 66(2): 641-653.

Vouillamoz, J.M. et al., 2012. Quantifying aquifer properties and freshwater resource in coastal barriers: A hydrogeophysical approach applied at Sasihithlu (Karnataka state, India). Hydrology and Earth System Sciences, 16(11): 4387-4400.

Werner, A.D. et al., 2013. Seawater intrusion processes, investigation and management: Recent advances and future challenges. Advances in Water Resources, 51(0): 3-26.